

C7orf30 specifically associates with the large subunit of the mitochondrial ribosome and is involved in translation

Bas F. J. Wanschers^{1,2}, Radek Szklarczyk¹, Aleksandra Pajak³,
Mariël A. M. van den Brand², Jolein Gloerich⁴, Richard J. T. Rodenburg²,
Robert N. Lightowlers³, Leo G. Nijtmans² and Martijn A. Huynen^{1,*}

¹Centre for Molecular and Biomolecular Informatics, Radboud University Nijmegen Medical Centre, The Netherlands, ²Nijmegen Centre for Mitochondrial Disorders at the Dept. of Pediatrics, Radboud University Nijmegen Medical Centre, The Netherlands, ³Mitochondrial Research Group, Institute for Ageing and Health, Newcastle University, Newcastle Upon Tyne NE2 4HH, UK and ⁴Nijmegen Proteomics Facility, Radboud University Nijmegen Medical Centre, The Netherlands

Received September 28, 2011; Revised December 2, 2011; Accepted December 7, 2011

ABSTRACT

In a comparative genomics study for mitochondrial ribosome-associated proteins, we identified C7orf30, the human homolog of the plant protein iojap. Gene order conservation among bacteria and the observation that iojap orthologs cannot be transferred between bacterial species predict this protein to be associated with the mitochondrial ribosome. Here, we show colocalization of C7orf30 with the large subunit of the mitochondrial ribosome using isokinetic sucrose gradient and 2D Blue Native polyacrylamide gel electrophoresis (BN-PAGE) analysis. We co-purified C7orf30 with proteins of the large subunit, and not with proteins of the small subunit, supporting interaction that is specific to the large mitoribosomal complex. Consistent with this physical association, a mitochondrial translation assay reveals negative effects of C7orf30 siRNA knock-down on mitochondrial gene expression. Based on our data we propose that C7orf30 is involved in ribosomal large subunit function. Sequencing the gene in 35 patients with impaired mitochondrial translation did not reveal disease-causing mutations in C7orf30.

INTRODUCTION

Relatively few proteins are known to be involved in the assembly of mitochondrial ribosomes. This stands in strong contrast to cytosolic ribosomes, where

approximately 200 factors have been predicted to participate in the biogenesis (1–3). Recently, ERAL1 (4,5) an RNA chaperone protein involved in the assembly of the small subunit and the guanosine triphosphatase (GTPase) NOA1 (6) have been found to function in the biogenesis of mitochondrial ribosomes. Identification of such factors is necessary to understand the ribosome assembly process and to resolve yet unexplained combined oxidative phosphorylation deficiencies (7).

In a comparative genomics-driven search for novel mitochondrial ribosome-associated proteins in human we identified C7orf30, a member of the iojap protein family that was previously identified as one of the most common protein families with an unknown function (8). First described in 1924 (9), the name iojap has been derived from the mutated maize *Iodent japonica* that has a characteristic white striping on its leaves. The striping is caused by failure of chloroplast development due to a mutation in a nuclear encoded gene (10). The causal mutation was identified in the so-called iojap locus (11) and has been implicated in the stability of chloroplast ribosomes, as iojap deficient plastids contain no ribosomes or high-molecular-weight RNAs (12). A physical link with the ribosome has been found in bacteria, where the iojap ortholog ybeB was found to co-migrate exclusively with the mature large 50S particle of *Escherichia coli* (13) and to be absent from the small subunit and the complete ribosome (14). Additionally, multiple protein components of the large ribosome (bacterial orthologs of human MRPL12, MRPL14 and MRPL19) have been co-purified with the bacterial iojap ortholog (15). Despite the wide phylogenetic distribution of the iojap family no deletion

*To whom correspondence should be addressed. Tel: +31 24 3619543; Fax: +31 24 3619395; Email: huynen@cmbi.ru.nl

The authors wish it to be known that, in their opinion, the first two authors should be regarded as joint First Authors.

phenotype could be identified in bacteria (14,16). In mammalian cells evidence for a C7orf30-ribosome association comes from the analysis of affinity purifications of ICT1 (a member of the mammalian mitoribosomal large subunit) where C7orf30 and many mitoribosomal subunits were co-isolated (17).

We set out to investigate the function of C7orf30. We confirm its mitochondrial localization and establish a specific association with the large subunit of the mitochondrial ribosome. We also show that a small interfering RNA (siRNA) knock-down of C7orf30 negatively affects the mitochondrial translation process. Our results are consistent with a role of C7orf30 in ribosomal large subunit assembly or translation initiation.

MATERIAL AND METHODS

Cloning and generation of expression plasmids

The *C7orf30* and *MRPL12* gene were polymerase chain reaction (PCR) amplified from a human heart complementary DNA (cDNA) library adding *Attb*-recombination sites (underlined) at the 5'- and 3'-end of the PCR product. The following primers were used: *C7orf30* forward: (5'-AAAAAGCAGGCTTCGCCACCATGGG GCCGGGCGGCCGTGTGG),

C7orf30 reversed: (5'-AGAAAGCTGGGTGTTTAC ATTTAACTCCACTGG-3'). *MRPL12* forward: (5'-AAAAGCAGGCTTCGCCACCATGCTGCCGGCGG CCGCTCGC-3'), *MRPL12*-reversed: (5'-AGAAAGC TGGGTGCTCCAGAACCACGGTGCCGCCAC-3').

Specific PCR products from the first PCR were subjected to a second round of PCR with adaptor primers: forward (5'-GGGGACAAGTTTGTACAAAAAAGCA GGCT-3') and reversed (5'-GGGGACCACTTTGTAC AAGAAAGCTGGGT-3') completing the *Attb* recombination sites. The PCR product of this second PCR was recombined in the pDONR201 vector using the Gateway BP clonase enzyme mix (Invitrogen). Next the pDONR201 constructs were recombined with a mammalian expression vector under the control of a tetracycline inducible promoter with the use of the LR clonase enzyme mix (Invitrogen) factors, adding green fluorescent protein (GFP) and a calmodulin-streptavidin tandem affinity purification (TAP) tag to the C-terminus. All constructs were verified by sequence analysis.

The production of ICT1- and MRPS27-FLAG constructs are described in (17).

Cell culture and generation of stable cell lines

T-RExTM Flp-InTM Human embryonic Kidney 293 cells (HEK293; Invitrogen) were grown and maintained in Dulbecco's modified Eagle medium (DMEM; Biowhitaker) supplemented with 10% [v/v] fetal calf serum (PAA Laboratories) and 1% [v/v] penicillin/streptomycin (GIBCO, Carlsbad, CA, USA), zeocin (300 µg/ml; Invitrogen) and 5 µg/ml blasticidin (Calbiochem). For the generation of stable C7orf30-GFP, C7orf30-TAP and MRPL12-TAP expressing cell lines constructs were transfected into HEK293

cells using Superfect transfection reagent (Qiagen). Selection for stable transfectants was achieved by replacing the zeocin in the culture medium for hygromycin (Calbiochem), final concentration 200 µg/ml. Gene expression was induced by adding doxycycline (Sigma) to the culture medium with a final concentration of 1 µg/ml for a minimum of 24 h. Rho0 cells were derived from 143B osteosarcoma cells and cultured, including a C73 fibroblast control as described in (18).

Immunofluorescence assay

HeLa cells were seeded and grown on glass cover slips before being fixed with 1% [w/v] paraformaldehyde in phosphate-buffered saline (PBS) and permeabilized with 0.4% Triton X-100 in PBS containing 3% bovine serum albumin (BSA). After permeabilization, samples were blocked with 3% BSA in PBS and incubated with anti-C7orf30 (dilution 1:200; Sigma) and anti-MRPL12 (dilution 1:500; Santa Cruz) antibodies followed by an incubation with secondary Alexa-555 and Alexa-488 conjugated secondary goat-anti-rabbit or anti-mouse antibodies (dilution: 1:1,000; Jackson Immunoresearch Laboratories), respectively. Nuclei were stained with Hoechst (Sigma). Finally, cover slips were washed with water and mounted on glass slides by inversion over Dako fluorescent mounting medium (Dako). Images were acquired with a Zeiss LSM 510 meta confocal laser scanning microscope.

siRNA transfections

A mix of four siRNAs was obtained from Thermo Scientific targeting *C7orf30* with the following siRNAs: 5'-GCAGCAUGGUGAUUCAUUU-3', 5'-UGACCCU CAUGUUAAGAU-3', 5'-CCAAGUUUGACAUCGA UAU-3', 5'-UGACCAGUUAGCUCAGAU-3'. For transfection HEK293 cells were seeded in six-well plates in culture medium without antibiotics at 50% confluency. Next day cells were transfected with the four *C7orf30* targeting duplexes using Dharmafect transfection reagent 1 (Dharmafect) in Optimem (Gibco). Final concentration of the siRNAs was 10 nM. As control mock-transfected cells were used. After 48 h cells were split one in six and transfected again the next day. Ninety-six hours after the first transfection, cells were harvested by trypsinization and processed for western blot analysis and/or used in a mitochondrial translation assay.

Sodium dodecyl sulfate-polyacrylamide gel electrophoresis, 1D and 2D Blue-Native PAGE western blotting and immunodetection

1D 3-13% gradient and 2D Blue Native polyacrylamide gel electrophoresis (PAGE) were done as described previously (19). For sodium dodecyl sulfate (SDS)-PAGE proteins samples were diluted once with Tricine sample buffer (Biorad) with 2% [v/v] 2-mercaptoethanol added and resolved with standard PAGE techniques. After electrophoresis resolved proteins were transferred to a polyvinylidene fluoride (PVDF) or nitrocellulose membrane by western blotting. After blocking with 5% non-fat dry milk in PBS with 0.1% [v/v] Tween-20 (PBST)

membranes were incubated with primary antibodies. Antibodies used: rabbit polyclonal anti-C7orf30 (dilution 1:2500; Sigma) anti-GFP [dilution 1:5000; (20)] anti-CBP for detection of the TAP-tag (dilution 1:1000; GenScript), anti-MRPS18B (dilution 1:1000 Protein tech), anti-MRPL3 (dilution 1:1000; Abcam), anti-MRPS22 (dilution 1:500; Proteintech) and anti-MRPL49 (dilution 1:2000; Proteintech), mouse monoclonal anti-SDHA (dilution 1:1000, MitoSciences), anti-Cox1 (dilution 1:1000, MitoSciences), anti-Cox2 (dilution 1:1000, MitoSciences) anti-TOM20 (dilution 1:5000, BD transduction laboratories) anti-CK-B 21E10 [dilution 1:5000; (21)] anti-MRPL12 antibody (dilution 1:1000; Abcam) and chicken anti-MRPL28 antibody (dilution 1:1000, Abcam). Primary incubations were followed by incubations with secondary horse radish peroxidase-conjugated goat anti-mouse, anti-rabbit (dilution: 1:1000; Invitrogen) or anti-chicken (dilution: 1:5000; SouthernBiotech) immunoglobulin Gs (IgGs). Immunoreactive bands were visualized using the enhanced chemiluminescence kit (Thermo Scientific) and detected with the Chemidoc XRS+ system (Biorad) and quantified with the provided Image Lab software.

Cellular fractionation and proteinase K protection assay

Cellular fractionation was carried out as described before (22). Permeabilization of mitochondria with digitonin followed by a proteinase K protection assay was performed like before (23). Susceptibility of proteins to degradation by proteinase K was assayed with SDS-PAGE followed by western blotting and probing the membranes with specific antibodies.

Isolation of mitoplasts and determination of protein concentrations

Cells were washed once with PBS, harvested, pelleted and resuspended in 100 μ l of ice-cold PBS to which an equal volume of 4% [w/v] digitonin in PBS was added. After a 10-min incubation on ice, 1 ml of ice-cold PBS was added to inactivate the digitonin and centrifuged for 10 min at 10 000g at 4°C. Finally, the mitochondrial enriched pellet was washed twice with ice-cold PBS to remove traces of digitonin. To solubilize mitochondrial proteins, the pellet was resuspended in 100 μ l AC/BT buffer (1.5 M aminocaproic acid, 75 mM bis-tris, pH 7.0) to which 10 μ l 20% lauryl maltoside [w/v] was added and incubated 10 min on ice. After this incubation the samples were centrifuged for 30 min at 10 000g. The supernatants containing the solubilized proteins were used for further analysis. Protein concentrations of the samples were determined with the microBCA protein kit (Thermo Scientific).

Affinity purifications and Fourier transform mass spectrometry analysis

HEK293 were induced for 3 days, harvested, resuspended in lysis buffer (30 mM Tris-HCl, 150 mM NaCl, 2% [v/v] lauryl maltoside) and freeze-thawed three times. Next lysates were spun-down for 10 min at 10 000g after which they were incubated in the presence of Streptactin

beads (IBA) for 2 h at 4°C under rotation. After the incubation beads were washed six times with washing buffer (30 mM Tris-HCl, 150 mM NaCl, 0.1% [v/v] lauryl maltoside) and bound proteins eluted in washing buffer with desbiotin (IBA). Finally the eluate was concentrated by passing it over a 3-kDa cut-off filter (Millipore) before being further processed for western blot or Fourier transform mass spectrometry (FT/MS) analysis as described in ref. 24. Affinity purifications and elution of FLAG peptides were performed like before (17).

Isokinetic sucrose gradient analysis of mitochondrial ribosomes

Isolated mitochondria (0.5–0.7 mg) or eluted immunoprecipitates were loaded on a linear sucrose gradient (1 ml 10–30% [v/v]) in 50 mM Tris-HCl pH 7.2, 10 mM Mg(OAc)₂, 40 mM NH₄Cl, 0.1 M KCl, 1 mM phenylmethylsulfonyl fluoride (PMSF), 50 μ g/ml chloramphenicol and centrifuged for 2 h 15 min at 100 000g at 4°C. Fractions (100 μ l) were collected and 10- μ l aliquots taken directly for analysis by western blot with antibodies directed against the mitoribosomal large subunit (MRPL3, Abcam ab39268), small subunit (MRPS18B, PTG labs 16139-1-AP), DAP3 (death-associated protein 3) or C7orf30 as described.

Mitochondrial translation analysis

In vivo mitochondrial protein synthesis in cultured cells was analyzed as described previously (25). Briefly, cells transfected with siRNAs targeting *C7orf30* and a mock control were labeled for 60 min in L-methionine and L-cysteine free DMEM supplemented with 10% dialyzed fetal calf serum (FCS), emetine (100 μ g/ml) to block cytosolic translation and 200 μ Ci/ml [³⁵S]-methionine and [³⁵S]-cysteine (Tran³⁵S-Label; MP Biomedicals, Eindhoven, The Netherlands). After labeling cells were chased for 10 min in regular DMEM with 10% FCS, harvested and resuspended in PBS containing 2% [w/v] lauryl maltoside. Insoluble material was removed from the lysate by centrifugation for 10 min at 10 000g. Equal amounts of protein were separated by SDS-PAGE on a 16% gel after which the gel was dried and exposed to a Phosphorimager screen. To visualize labeled proteins the screen was scanned with a FLA5100 scanner (Fujimager, Tilburg, The Netherlands). To confirm equal loading of proteins the gel was rehydrated and stained with Coomassie Brilliant Blue G-250. Mitochondrial translation was inhibited by adding chloramphenicol (CAP), final concentration 40 μ g/ml, to the medium for 72 h.

Identification of a C7orf30 ortholog in *Blastocystis hominis*

Blastocystis hominis possesses mitoribosomes but lacks mitochondrial adenosine triphosphatase (ATPase) previously linked to *C7orf30* function (26). The *C7orf30* gene appears to be absent from *B. hominis* gene catalog. To find the gene in the genomic sequence we used the PFAM domain DUF143 (27) and carried out profile-DNA search against the *B. hominis* genome (28). Nucleotide positions 801783-801490 of contig 137 (CABX01000137.1)

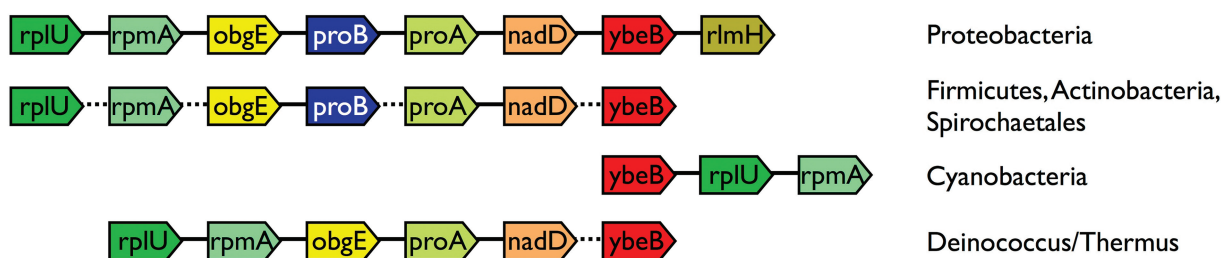


Figure 1. Conservation of the bacterial operon that contains the bacterial ortholog of *C7orf30*, *ybeB*. The gene order is conserved in divergent branches of bacteria. Solid lines connect neighboring genes in the genomes of the given clade (right), a dotted line is used if both genes are not direct neighbors, but include other genes in between. *rplU*, ribosomal protein L21; *rpmA*, ribosomal protein L27; *obgE*, GTPase; *proB*, glutamate 5-kinase; *proA*, gamma-glutamyl phosphate reductase; *nadD*, nicotinic acid mononucleotide adenyltransferase; *ybeB*, *C7orf30* homolog; *rlmH*, 23S rRNA methyltransferase. Data from the STRING database (39).

encode a putative ortholog of the *C7orf30* gene (E-value = $1e-10$). Furthermore, the search with the predicted *B. hominis* *C7orf30* protein against the database of eukaryotic protein sequences retrieves an annotated DUF143-containing protein in *Naegleria gruberi* (XP_002678819.1, E-value < $3e-4$), supporting the presence of the *C7orf30* ortholog in *B. hominis* genome.

Maximum likelihood phylogenetic analysis

An alignment of *C7orf30* homologs from two proteobacterial, two cyanobacterial and eukaryotic species was created with Clustal-W (29). To construct the tree, the conserved domain (DUF143) was selected and columns containing gaps were removed. The Maximum Likelihood phylogeny was computed with PhyML 3.0 (30), using the LG amino acid substitution model with a gamma distribution approximated by four discrete-rate categories (4G). The proportion of invariant sites (I), the gamma shape parameter (alpha) and amino acid frequencies were estimated from the data, as implemented in ProtTest 3.0 (31).

RESULTS

Bacterial orthologs of *C7orf30* occur in a ribosomal large subunit (assembly) operon

The *E. coli* ortholog of the human *C7orf30* gene, *ybeB*, belongs to a conserved operon that encodes bacterial orthologs of ribosomal proteins L21 and L27 (Figure 1). The gene order is a remarkably well conserved, not only in the α -proteobacteria (the genus that gave rise to mitochondria), but also in the bacterial clades Actinobacteria, Cyanobacteria (ancestors of the chloroplasts), Firmicutes as well as Deinococci (Figure 1). Besides *ybeB*, four other proteins encoded in the operon have specifically been implicated in the large subunit of the bacterial ribosome: two that are subunits of the ribosomal large subunit (*rplU* and *rpmA*), the *obgE* GTPase that is involved in the large subunit assembly (32), and a 23S rRNA methyltransferase [*rlmH*, (33,34)]. Of these, *rpmA* (ribosomal protein L27) is added to the ribosomal large subunit late in the ribosome assembly, while the other

proteins function specifically in the mature form of the complex (13,14,32–37).

A genomic link of *C7orf30* orthologs to (di)nucleotide metabolism

Aside from genes for ribosomal (assembly) proteins, the conserved operon also contains metabolic genes *nadD* (nicotinic acid mononucleotide adenyltransferase), *proB* and *proA* (gamma-glutamyl kinase and NADPH-dependent phosphate reductase respectively, genes that participate in the metabolism of glutamate). The link with *nadD* is specifically strong, as *ybeB* can even be found fused with it, providing the strongest genomic indication of functional link between proteins (38). The *nadD* and *ybeB* fusion has occurred multiple times independently in bacterial evolution: in *Pedobacter heparinus* (Bacteroidetes), *Solibacter usitatus* (Acidobacteria), *Clostridium phytofermentans* (Firmicutes) and in the *Rhodococcus* and *Coriobacteriaceae* lineages (Actinobacteria) [data from (39)]. The *nadD* gene product catalyzes the adenylation of nicotinate mononucleotide (NaMN) to nicotinic acid adenine dinucleotide as a part of NAD(P) biosynthesis (40). Further hints for a possible role of the bacterial *C7orf30* orthologs in (di)nucleotide metabolism come from its three-dimensional (3D) structure that has been determined for two *C7orf30* orthologs (PDB:2id1 and PDB:2o5a, see Figure 2A). This allowed the classification of the proteins as a *Beta Polymerase domain 2* [CATH 3.30.460.10, (41)], showing structural homology with DNA and RNA polymerases, transfer RNA (tRNA) processing, messenger RNA (mRNA) polyadenylation proteins as well as multiple nucleotidyltransferases. Hence, both gene fusion and structural classification of the *C7orf30* protein fold independently point to its role in (di)nucleotide metabolism (Figure 1).

The bacterial *C7orf30* orthologs have evolutionary attributes of ribosomal subunits and translation factors

The bacterial *C7orf30* ortholog, together with genes encoding 21 ribosomal proteins and translation factors, has been found to be ‘untransferrable’ between bacterial species (42). Additionally, the *C7orf30* orthologs are universally single copy genes, occurring in bacteria in exactly one copy per genome (42), congruent with ribosomal

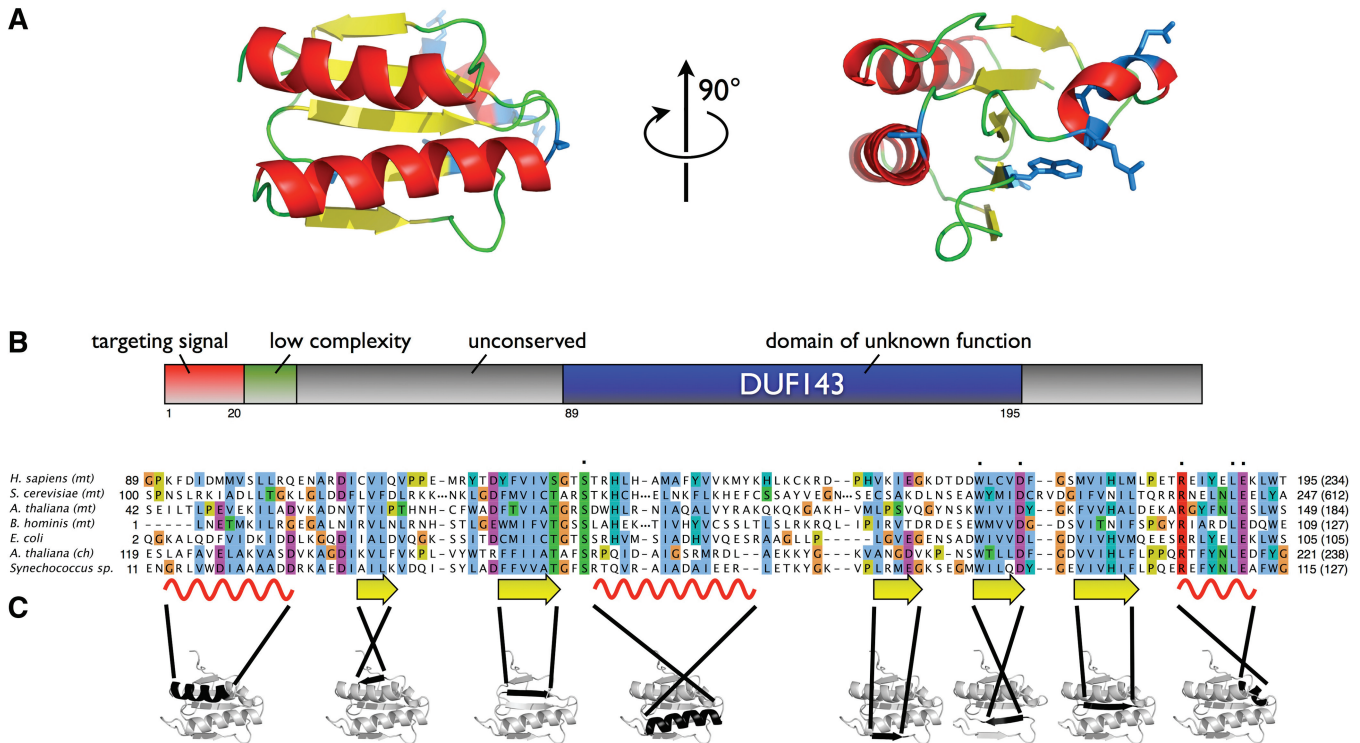


Figure 2. Domain composition of the human C7orf30 protein. (A) Predicted structure of the conserved DUF143 domain modeled after the *Bacillus halodurans* ortholog (pdb:2o5a, Benach *et al.*, submitted for publication). Homology model was created with WHAT IF (54) and visualized with PyMOL 1.3 (<http://www.pymol.org>). Side chains of residues conserved in all orthologs are shown in blue. (B) Functional domains of the human C7orf30 protein. N-terminal targeting signal was predicted with Target P (44). Bacterial homologs possess only the DUF143 domain. (C) Multiple alignment and secondary structure of the conserved DUF143 domain. Non-conserved insertions in *S. cerevisiae* and *B. hominis* are replaced with dots. Mitochondrial and chloroplast proteins are marked with *mt* and *ch*, respectively. The alignment was visualized using Jalview (55) using the Clustalx color scheme. Residues conserved in all orthologs are marked above the alignment. Secondary structure α -helix (red) and β -sheet (yellow) regions are marked beneath the alignment together with their position in the homology model of C7orf30. See Figure 2 for the list of species used in the alignment.

subunits and translation factors (see Supplementary Data). Next to the C7orf30 orthologs, only ribosomal and ribosome-associated proteins have the properties of being horizontal gene transfer-resistant and having a single-copy genomic presence. These genetic attributes of the C7orf30 orthologs and their congruence with ribosomal subunits strongly support a role of the protein in the ribosome.

The phylogenetic distribution of C7orf30 orthologs

Next to being part of a conserved operon that encodes two ribosomal proteins, a functional association between C7orf30 orthologs and ribosomes is also suggested by the gene's phylogenetic distribution. The gene is present in bacteria as well as eukaryotes with mitochondria, but absent from species that lack ribosomes of bacterial origin. The gene is absent in Archaea and has been lost independently multiple times in eukaryotes that do not possess a mitochondrial genome. We find that all mitochondria-less fully sequenced eukaryotes (from *Cryptosporidia*, *Trichomonas*, *Entamoeba*, *Giardia* and *Encephalitozoon* clades) lack a gene encoding a C7orf30 ortholog. In contrast, we detected an ortholog of the gene in *Blastocystis hominis* (see Figure 2C and 'Materials and Methods' section), a species that possesses

mitochondrial ribosomes but lacks the ATP synthase. Thus the previously reported ATP9-specific function of the *Saccharomyces cerevisiae* ortholog of C7orf30 (26) may be limited to the fungal clade.

The eukaryotic proteins from the C7orf30 family can be twice as long as the bacterial orthologs. The N- and C-terminal extensions, including a mitochondrial targeting signal, are however poorly conserved among the eukaryotes (see Figure 2B for the domain composition). Additionally in eukaryotes, unlike in bacteria, C7orf30 orthologs can be found in two copies per genome. Two copies are present in genomes of species with DNA-containing plastids. In *Arabidopsis thaliana*, the iojap protein (encoded by the AT3G12930 gene) inherited from cyanobacteria (Figure 3) localizes to the chloroplast (43), and has a chloroplast N-terminal localization signal (TargetP score 0.9) (44). The second plant iojap protein (encoded by the AT1G67620 gene) contains a predicted mitochondrial targeting signal (TargetP score 0.7). The mitochondrial localization is consistent with the phylogenetic clustering of the protein with α -proteobacterial orthologs (see Figure 3). Two iojap genes can also be found in the apicomplexan species *Toxoplasma gondii* that contains both mitochondria and plastids. The apicomplexan plastids result from a secondary

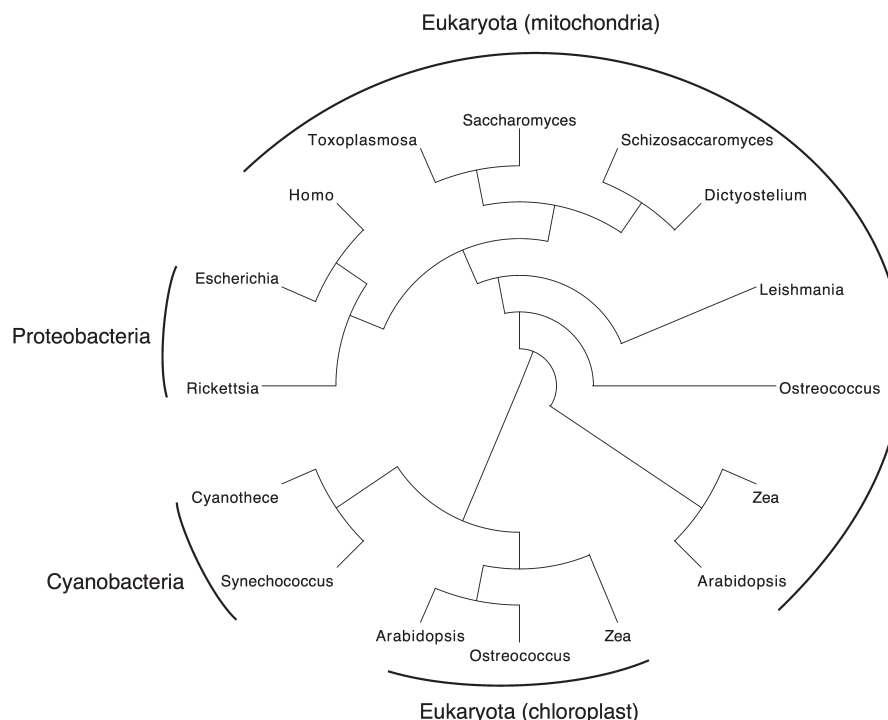


Figure 3. Maximum likelihood phylogeny (see ‘Materials and Methods’ section for details) of *C7orf30* homologs reveals distinct chloroplast/cyanobacterial and mitochondrial/proteobacterial clusters. Species included: *Rickettsia prowazekii*, *Escherichia coli*, *Toxoplasma gondii*, *Blastocystis hominis*, *Leishmania major*, *Saccharomyces cerevisiae*, *Ostreococcus lucimarinus*, *Dictyostelium discoideum*, *Schizosaccharomyces pombe*, *Homo sapiens*, *Zea mays*, *Arabidopsis thaliana*, *Synechococcus* sp. PCC 7002 and *Cyanotheca* sp. PCC 7424.

endosymbiosis and lack an ATPase, including ATP9 (45), providing further support that *C7orf30* is not functionally linked with ATPase in eukaryotes in general.

***C7orf30* is a mitochondrial localized protein**

Mitochondrial targeting prediction programs [Mitoprot (46) and TargetP, (44)] predict a mitochondrial localization of *C7orf30*. To test these predictions, immunofluorescence studies using HeLa cells were performed showing that *C7orf30* colocalizes with MRPL12, a protein of the large subunit of the mitochondrial ribosome (Figure 4A). The mitochondrial localization of *C7orf30* was further substantiated by western blot analysis of fractionated cells, revealing a strong, specific signal for *C7orf30* at 24 kDa in the crude mitochondrial fraction as confirmed by the presence of the mitochondrial outer membrane localized TOM20. No signal was detected in the cytosolic fraction (Figure 4B).

To determine *C7orf30*'s submitochondrial localization, proteinase K protection assays were performed using mitochondria with digitonin-permeabilized outer membranes in the absence or presence of membrane dissolving Triton X-100. This approach showed resistance of *C7orf30* to proteinase K similar to matrix-localized SDHA, whereas both TOM20 (a mitochondrial outer membrane protein) and, to a lesser extent, prohibitin 1 (an inner membrane protein) are susceptible to digestion in the absence of Triton X-100. Only after dissolving the outer and inner membrane, do *C7orf30* and SDHA

become degraded by proteinase K (Figure 4C). These results point towards a localization of *C7orf30* within the boundaries of the mitochondrial inner membrane.

***C7orf30* is not detectable in cells devoid of mitochondrial DNA**

We tested human cells deprived of mitochondrial DNA (mtDNA; Rho0 cells) for the presence of the *C7orf30*. In contrast to control cell lines, *C7orf30* was not detected in Rho0 cells (Figure 4D). Next, we investigated whether the CAP inhibition of mitochondrial protein synthesis affects *C7orf30* protein levels. Whereas mitochondrially encoded Cox2 levels are severely decreased upon treatment with CAP and return to normal levels 24 h after CAP removal, *C7orf30* and SDHA levels remain unaffected (Figure 4E). Taken together, these results suggest that the stability of *C7orf30* does not depend on the presence of mitochondria-encoded proteins, but rather on the mtDNA itself or on mitochondria-encoded rRNAs or tRNAs.

***C7orf30* associates with the mitochondrial ribosome large subunit**

The above-mentioned analysis of *C7orf30* and its orthologs point towards a functional link with the mitochondrial ribosome. To investigate a possible structural link with the ribosome 2D Blue Native PAGE analysis

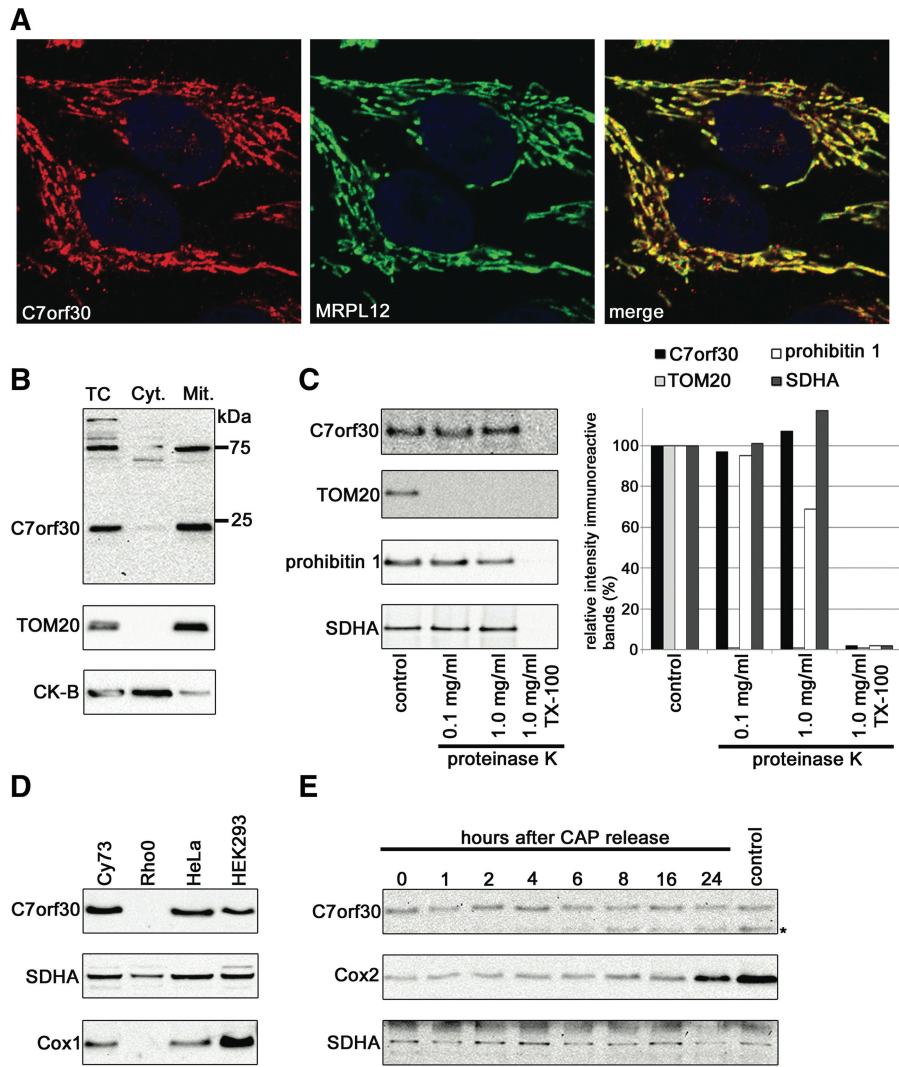


Figure 4. C7orf30 is a mitochondrial matrix localized protein absent in cells without mitochondrial DNA. (A) Confocal microscope analysis of HeLa cells immunostained with anti-C7orf30 (left panel) and anti-MRPL12 (middle panel) antibodies. The merged image is shown on the right. Nuclei are counterstained with Hoechst. (B) Cellular fractionation of HEK293 cells. Total cell lysate (TC), cytosolic (Cyt.) and mitochondrial (Mit.)-enriched fractions were analyzed using western blotting with indicated antibodies. As control of mitochondrial and cytoplasmic fractions TOM20 (mitochondrial outer membrane) and anti-CK-B (Creatine kinase B-type) antibodies were used, respectively. The 75-kDa signal after C7orf30 antibody incubation presumably corresponds to a cross-reacting contaminant. (C) C7orf30 resides within the boundaries of the mitochondrial inner membrane. Mitochondria with digitonin permeabilized outer membranes were subjected to the amounts of proteinase K indicated, in the absence or presence of membrane dissolving Triton X-100 (TX-100). Susceptibility of proteins to degradation was analyzed with western blotting using indicated antibodies; TOM20: mitochondrial outer membrane, prohibitin 1: intermembrane space facing protein, SDHA: matrix. Quantification of the immunoreactive bands is indicated at the right. (D) C7orf30 is not detectable in cells devoid of mitochondrial DNA. SDS-PAGE analysis of fibroblast Cy73, mitochondrial DNA less (Rho0), HeLa and HEK293 cells. Membranes were probed with the antibodies indicated. Cox1 (mitochondrial encoded) and SDHA (nuclear encoded) were used as controls. (E) Inhibition of mitochondrial translation does not affect C7orf30 protein levels. Mitochondrial translation was inhibited with chloramphenicol (CAP) and allowed to resume again for an increasing amount of time. Protein levels were analyzed with SDS-PAGE followed by western blotting. Immunostainings for Cox2 (mitochondrial encoded) and SDHA were used as controls. Asterisk indicates remaining Cox2 signal.

of C7orf30-GFP expressing cells was performed. Although a substantial part of C7orf30-GFP is present at low-molecular-weight complexes, a small fraction resides in a high-molecular-weight complex, co-localizing with ribosomal subunits (Figure 5A). Studies using isokinetic sucrose gradient centrifugation show C7orf30 co-sedimenting with the ribosomal large subunit protein MPRL3 in fractions 5 and 6 (Figure 5B). The small subunit protein MRPS18B is most abundant in fraction 4, where C7orf30 is absent (Figure 5B). To confirm the

specificity of the co-localization, we immunoprecipitated ribosomes with an antibody against ICT1-FLAG, a mitochondrial large ribosomal subunit protein (17) and loaded them on a sucrose gradient. This experiment reveals co-sedimentation of C7orf30 with the large ribosomal subunit associated pool of MRPL3 and not with the small ribosomal subunit protein MRPS18B (Figure 5C). C7orf30 is also not detectable in more dense fractions of the sucrose gradient (Figure 5C). Consistently, in another experiment with a sucrose gradient loaded with a small

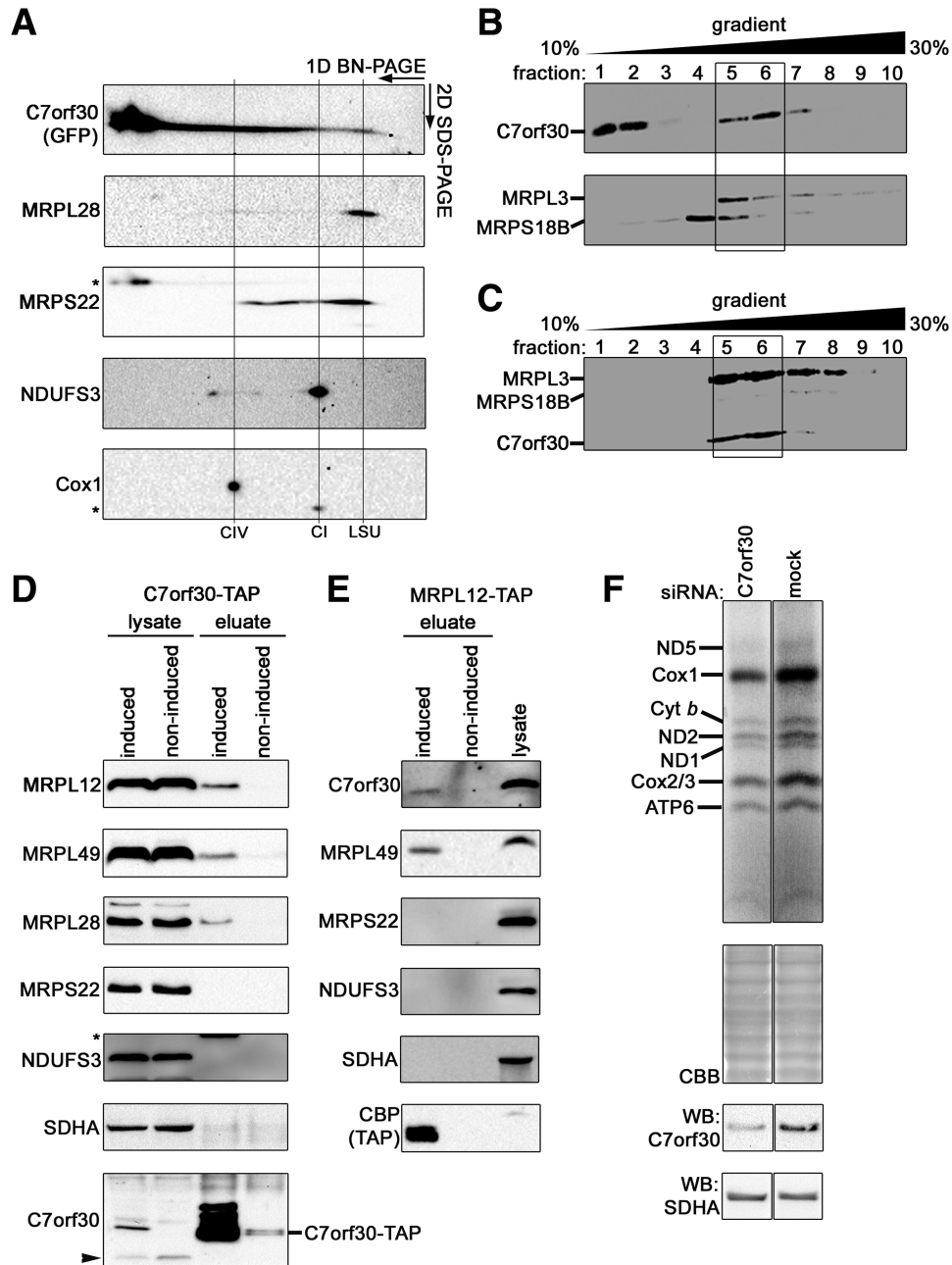


Figure 5. C7orf30 associates with the large subunit of the mitochondrial ribosome and is important for mitochondrial translation. (A) Two-dimensional Blue Native PAGE analysis of C7orf30-GFP. Mitochondrial lysate of HEK293 expressing C7orf30-GFP was subjected to separation in the first and second dimension under native and denaturing conditions, respectively before western blot analysis with indicated antibodies. The vertical lines indicate the position of the large subunit (LSU), complex I (CI) and complex IV (CIV). Asterisk denotes signal from previous incubation. (B) Western blot analysis of an isokinetic sucrose gradient centrifugation (see ‘Materials and Methods’ section) immunostained for C7orf30. To indicate the positions of the mitochondrial ribosomal subunits the membranes were additionally stained for MRPL3 and MRPS18B, representing the large subunit and small subunit respectively (lower panel). Although the two subunits have a similar mass, MRPL3 migrates slightly more slowly on SDS-PAGE and can be seen in fractions 5, 6. (C) C7orf30 co-sediments with the large subunit bound pool of ICT1. HEK293 expressing ICT1-FLAG (large subunit protein) were subjected to immunoprecipitation with FLAG-antibody followed by elution of bound proteins. The entire eluate was separated by isokinetic sucrose gradient centrifugation before Western blot analysis with indicated antibodies. (D and E) Western blot analysis of C7orf30-TAP (D) and MRPL12-TAP (E) affinity purifications. Used antibodies are indicated on the left. As control noninduced cells were used. Efficiency of the C7orf30-TAP pull down was assessed by probing the blots with anti-C7orf30 (lower panel). The arrow indicates the signal for endogenous C7orf30, asterisk the signal from a previous incubation. MRPL12-TAP purification was assessed by probing the blots with anti-CBP antibody recognizing the TAP-tag. SDHA and NDUFS3 were used as control to rule out a-specific protein binding. (F) Metabolic labeling of mitochondrial translation products with ³⁵S in HEK293 cells transfected with siRNAs targeting C7orf30 and the mock control. Mitochondrial translation products are indicated on the left. Equal loading of the gels was confirmed by rehydrating and staining the gel with Coomassie Brilliant Blue G-250 (CBB). Knock-down of proteins was verified by western blot (WB) and probing the membranes with indicated antibodies. SDHA was used as loading control.

subunit MRPS27-FLAG immunoprecipitate both MRPL3 and C7orf30 are not detected (Supplementary Figure SI1). Taken together, these data strongly support that C7orf30 associates with the large and not the small mitoribosomal subunit.

FT/MS analysis of TAP-tagged C7orf30 protein purifications identifies components of the large ribosome MRPL12 and MRPL49 as co-purifying proteins (Supplementary Table SI2). To verify these interactions, C7orf30- and MRPL12-TAP purifications were analyzed with western blots, confirming the association (Figure 5D and E). Immunostaining reveals co-purification of all tested ribosomal large subunit protein components (MRPL12, 28, 49). MRPS22, the protein component of the ribosomal small subunit, could not be detected in the eluate, corroborating the specific association between C7orf30 and the large subunit. To exclude an α -specific protein binding to the beads the blot was additionally probed for NDUFS3 (complex I subunit) and SDHA (complex II subunit). Both proteins were not detected in the eluate, confirming the specificity of the purification. Efficiency of the C7orf30-TAP purification was determined by immunostaining for C7orf30, at the same time allowing us to look for co-isolation of endogenous C7orf30. As no C7orf30 was detected in the eluate we conclude that no dimerization or multimerization takes place (Figure 5D). Additionally, the interaction between C7orf30 and the ribosomal large subunit has been confirmed by TAP purification of MRPL12-TAP that retrieves C7orf30 and MRPL49 but not the small ribosomal subunit MRPS22 or other proteins tested (Figure 5E). Combined, these data argue for C7orf30 as a *bona fide* mitochondrial ribosomal large subunit binding protein.

Knock-down of C7orf30 affects mitochondrial translation

To investigate a possible role for C7orf30 in mitochondrial translation, metabolic labeling studies were performed using C7orf30 depleted HEK293 cells. After the C7orf30 siRNA knock-down, a decrease of mitochondrial translation products was observed compared to the control, most noticeable for Cox1 (Figure 5F, Supplementary Table SI1). These results suggest that C7orf30 is necessary for proper mitochondrial gene expression.

C7orf30 sequencing in patients

The coding sequence of C7orf30 gene has been sequenced in a cohort of 35 patients with combined complex I+III+IV deficiencies (i.e. with a biochemical signature of impaired mitochondrial translation). No pathogenic mutations in the gene have been found among the patients (data not shown).

DISCUSSION

In this study we identify C7orf30 as a novel the mitochondrial ribosome binding protein. Our results point towards a role in the ribosome large subunit, a function that is supported by the data from ref. 47. The conserved operon organization of the bacterial C7orf30 ortholog,

the gene's resistance to horizontal transfer between species as well as its universally single copy presence in bacterial genomes point to the gene's role in the ribosomal large subunit across the bacteria. Experimental results in *E. coli* (14) corroborate this observation. Genomic evidence from eukaryotes that encompasses (i) the correlated presence with the number of ribosomes of bacterial origin (no orthologs in genomes of amitochondriate eukaryotes to two copies in species with mitochondria and plastids) and (ii) the phylogenetic origin of C7orf30 orthologs that is consistent with the ribosome's origin (Figure 3) argue for a similar function of the protein in organellar ribosomes of eukaryotes, strengthened by the lack of functional ribosomes in maize chloroplasts with an affected *iojap* locus (12). Our results from the isokinetic sucrose gradient and C7orf30 affinity purifications are both in agreement with the association of the protein with the ribosomal large subunit.

The C7orf30 ortholog in *S. cerevisiae*, named *Atp25*, has been shown to play a role in ATPase translation and assembly (26). The yeast protein contains a C-terminal domain, absent outside the fungal evolutionary lineage, which is cleaved to function in stabilization of the *ATP9* mRNA. The DUF143 (C7orf30)-domain containing N-terminal part has been observed to be involved in the oligomerization of Atp9p, thereby playing an important role in the assembly of the F₁F₀ ATPase (26). We identify a C7orf30 ortholog in the genome of a eukaryotic species that lacks a mitochondrial F₁F₀ ATPase (*B. hominis*) and, in contrast, find a perfect correlation between the number of C7orf30 orthologs encoded in the nuclear genome and the number of cell's organellar genomes (0, 1 or 2). We conclude that the ATPase-related role of the protein may be limited to fungal species.

While no *ybeB* gene deletion phenotype has been observed in bacteria (14), C7orf30 knockdown impairs mitochondrial translation in human cells. This result argues for the proteins' involvement in maintaining ribosomal function. Its specific role in the ribosomal large subunit in bacteria has remained unknown. Attempts to produce recombinant *ybeB* in bacteria often fail, possibly due to intolerance of the host to increased dosage of the transferred gene in addition to the endogenous protein (42). Similarly, we observed that the induction of tagged C7orf30 does not lead to high levels of the fusion protein (Figure 5D), and at the same time negatively affects endogenous C7orf30 protein levels (Figure 5D). Both observations suggest that the cells keep C7orf30 protein levels under tight control, but it is not known how this regulation is executed.

Genomic presence-absence patterns of the C7orf30 orthologs in eukaryotes point to the evolutionary association between the protein and organellar ribosomes. The genomic association is recapitulated at the cellular level, as the western blot analysis of Rho0 cells reveals the absence of C7orf30 protein in this ribosome-lacking cell type (Figure 4D), further strengthening the functional link between C7orf30 protein and ribosomes. While the specific role of the association remains unclear, other genes that constitute the bacterial operon with C7orf30 ortholog *ybeB* suggest concerted involvement in the late

Table 1. The functional association of the proteins in the operon with the bacterial ribosome

| <i>E. coli</i> gene | Bacterial protein | | | Human orthologs |
|---------------------|---|------------------------------------|---|-------------------------------|
| | Description | Function in the bacterial ribosome | Associated with ribosomal large subunit | |
| <i>rplU</i> | Ribosomal protein L21 | Subunit | | MRPL21 |
| <i>rpmA</i> | Ribosomal protein L27 | Subunit | Mature | MRPL27 |
| <i>obgE</i> | GTPase ObgE/CgtA | Assembly | Mature | GTPBP5, OLA1, GTPBP10 |
| <i>proB</i> | Glutamate 5-kinase | | | ALDH18A1 |
| <i>proA</i> | Gamma-glutamyl phosphate reductase | | | ALDH18A1 |
| <i>nadD</i> | Nicotinic acid mononucleotide adenylyltransferase | | | NMNAT1, NMNAT2, NMNAT3 |
| <i>ybeB</i> | Uncharacterized homolog of plant iojap protein | Binding | Mature | C7orf30 |
| <i>rlmH</i> | 23S rRNA methyltransferase | rRNA modification | Mature | - |

Genes marked in bold encode proteins that are mitochondrial in human.

large subunit biogenesis, possibly at the moment of translation initiation. The involvement of the gene product in translation initiation would be congruent with the gene's bacterial universally single copy presence [specific to subunits and translation factors (42)] and the exclusive association with the complete large subunit of the ribosome. A similar mode of association, but with a ribosomal small subunit, has been observed for translation initiation factor IF-3 (14).

The composition of the bacterial operon suggests other human orthologs that may also play a role in large ribosome function. For example, the human GTPBP5 protein, the ortholog of bacterial *obgE* (Table 1), is involved in maturation of mitoribosomes (48). The other two *obgE* orthologs (OLA1/GTPBP9 and GTPBP10) are not very well studied in mammals, but constitute promising candidates for the function in the mitochondrial large ribosome.

Our experimental data do not provide an explanation for the 3D structure of bacterial C7orf30 orthologs, which is typical of nucleotidyltransferases, nor do they explain the occurrence of *nadD* [nicotinamide mononucleotide (NMN)-adenylyltransferase] in the same operon or even in a single gene. One explanation for the link of *nadD* with the ribosomal large subunit is its role in the (re)generation of NAD that is used for protein deacetylation by sirtuins, like the bacterial *cobB* (49). In *E. coli*, acetylation of the large ribosomal protein L12 subunit has specifically been shown to increase its interaction with the ribosomal stalk complex (50). In mitochondria, NAD-dependent deacetylation of the ribosomal large subunit MPL10 by SIRT3 has been implicated in regulating ribosomal activity (51). Nevertheless, we currently have no evidence that C7orf30 plays a role in this process, either directly via its interaction with the large ribosomal subunit or indirectly as a nucleotidyltransferase in NAD metabolism.

SUPPLEMENTARY DATA

Supplementary Data are available at NAR Online: Supplementary Tables 1 and 2, Supplementary Figure 1, Supplementary Methods and Supplementary References [52,53].

ACKNOWLEDGEMENTS

We want to thank Björn Fischer for helping with the confocal laser scanning microscope and Fenna Hensen for cloning the MRPL12-gene and generating the MRPL12-TAP expression construct and cell lines.

FUNDING

Horizon grant (050-71-053) from the Netherlands Organization for Scientific Research (NWO); the CSBR (Centres for Systems Biology Research) initiative from NWO (No: CSBR09/013V and by Biotechnology and Biological Sciences Research Council (grant number BB/F011520/1 to R.N.L.). Funding for open access charge: Radboud University Nijmegen Medical Centre.

Conflict of interest statement. None declared.

REFERENCES

- Fromont-Racine, M., Senger, B., Saveanu, C. and Fasiolo, F. (2003) Ribosome assembly in eukaryotes. *Gene*, **313**, 17–42.
- Kressler, D., Linder, P. and de La Cruz, J. (1999) Protein trans-acting factors involved in ribosome biogenesis in *Saccharomyces cerevisiae*. *Mol. Cell. Biol.*, **19**, 7897–7912.
- Saveanu, C., Namane, A., Gleizes, P.E., Lebreton, A., Rousselle, J.C., Noaillac-Depeyre, J., Gas, N., Jacquier, A. and Fromont-Racine, M. (2003) Sequential protein association with nascent 60S ribosomal particles. *Mol. Cell. Biol.*, **23**, 4449–4460.
- Dennerlein, S., Rozanska, A., Wydro, M., Chrzanowska-Lightowlers, Z.M. and Lightowlers, R.N. (2010) Human ERAL1 is a mitochondrial RNA chaperone involved in the assembly of the

- 28S small mitochondrial ribosomal subunit. *Biochem. J.*, **430**, 551–558.
5. Uchiyama, T., Ohgaki, K., Yagi, M., Aoki, Y., Sakai, A., Matsumoto, S. and Kang, D. (2010) ERAL1 is associated with mitochondrial ribosome and elimination of ERAL1 leads to mitochondrial dysfunction and growth retardation. *Nucleic Acids Res.*, **38**, 5554–5568.
 6. Kolanczyk, M., Pech, M., Zemojtel, T., Yamamoto, H., Mikula, I., Calvaruso, M.A., van den Brand, M., Richter, R., Fischer, B., Ritz, A. *et al.* (2011) NOA1 is an essential GTPase required for mitochondrial protein synthesis. *Mol. Biol. Cell*, **22**, 1–11.
 7. Smits, P., Smeitink, J. and van den Heuvel, L. (2010) Mitochondrial translation and beyond: processes implicated in combined oxidative phosphorylation deficiencies. *J. Biomed. Biotechnol.*, **2010**, 737385.
 8. Galperin, M.Y. and Koonin, E.V. (2004) ‘Conserved hypothetical’ proteins: prioritization of targets for experimental study. *Nucleic Acids Res.*, **32**, 5452–5463.
 9. Jenkins, M.T. (1924) Heritable characters of maize XX iojap-stripping, a chlorophyll defect. *J. Heredity*, **15**, 467–472.
 10. Rhoades, M.M. (1943) Genic induction of an inherited cytoplasmic difference. *Proc. Natl Acad. Sci. USA*, **29**, 327–329.
 11. Han, C.D., Coe, E.H. Jr and Martienssen, R.A. (1992) Molecular cloning and characterization of iojap (ij), a pattern striping gene of maize. *EMBO J.*, **11**, 4037–4046.
 12. Walbot, V. and Coe, E.H. (1979) Nuclear gene iojap conditions a programmed change to ribosome-less plastids in *Zea mays*. *Proc. Natl Acad. Sci. USA*, **76**, 2760–2764.
 13. Jiang, M., Datta, K., Walker, A., Strahler, J., Bagamasbad, P., Andrews, P.C. and Maddock, J.R. (2006) The *Escherichia coli* GTPase CgtAE is involved in late steps of large ribosome assembly. *J. Bacteriol.*, **188**, 6757–6770.
 14. Jiang, M., Sullivan, S.M., Walker, A.K., Strahler, J.R., Andrews, P.C. and Maddock, J.R. (2007) Identification of novel *Escherichia coli* ribosome-associated proteins using isobaric tags and multidimensional protein identification techniques. *J. Bacteriol.*, **189**, 3434–3444.
 15. Butland, G., Peregrin-Alvarez, J.M., Li, J., Yang, W., Yang, X., Canadien, V., Starostine, A., Richards, D., Beattie, B., Krogan, N. *et al.* (2005) Interaction network containing conserved and essential protein complexes in *Escherichia coli*. *Nature*, **433**, 531–537.
 16. Baba, T., Ara, T., Hasegawa, M., Takai, Y., Okumura, Y., Baba, M., Datsenko, K.A., Tomita, M., Wanner, B.L. and Mori, H. (2006) Construction of *Escherichia coli* K-12 in-frame, single-gene knockout mutants: the Keio collection. *Mol. Syst. Biol.*, **2**, 2006 0008.
 17. Richter, R., Rorbach, J., Pajak, A., Smith, P.M., Wessels, H.J., Huynen, M.A., Smeitink, J.A., Lightowlers, R.N. and Chrzanowska-Lightowlers, Z.M. (2010) A functional peptidyl-tRNA hydrolase, ICT1, has been recruited into the human mitochondrial ribosome. *EMBO J.*, **29**, 1116–1125.
 18. Corona, P., Antozzi, C., Carrara, F., D’Incerti, L., Lamantea, E., Tiranti, V. and Zeviani, M. (2001) A novel mtDNA mutation in the ND5 subunit of complex I in two MELAS patients. *Ann. Neurol.*, **49**, 106–110.
 19. Ugalde, C., Vogel, R., Huijbens, R., Van Den Heuvel, B., Smeitink, J. and Nijtmans, L. (2004) Human mitochondrial complex I assembles through the combination of evolutionary conserved modules: a framework to interpret complex I deficiencies. *Hum. Mol. Genet.*, **13**, 2461–2472.
 20. Cuppen, E., Wijers, M., Schepens, J., Fransen, J., Wieringa, B. and Hendriks, W. (1999) A FERM domain governs apical confinement of PTP-BL in epithelial cells. *J. Cell. Sci.*, **112** (Pt 19), 3299–3308.
 21. Sisternans, E.A., de Kok, Y.J., Peters, W., Ginsel, L.A., Jap, P.H. and Wieringa, B. (1995) Tissue- and cell-specific distribution of creatine kinase B: a new and highly specific monoclonal antibody for use in immunohistochemistry. *Cell Tissue Res.*, **280**, 435–446.
 22. Vogel, R.O., Janssen, R.J., Ugalde, C., Grovenstein, M., Huijbens, R.J., Visch, H.J., van den Heuvel, L.P., Willems, P.H., Zeviani, M., Smeitink, J.A. *et al.* (2005) Human mitochondrial complex I assembly is mediated by NDUFAF1. *FEBS J.*, **272**, 5317–5326.
 23. Duxin, J.P., Dao, B., Martinsson, P., Rajala, N., Guittat, L., Campbell, J.L., Spelbrink, J.N. and Stewart, S.A. (2009) Human Dna2 is a nuclear and mitochondrial DNA maintenance protein. *Mol. Cell. Biol.*, **29**, 4274–4282.
 24. Saada, A., Vogel, R.O., Hoefs, S.J., van den Brand, M.A., Wessels, H.J., Willems, P.H., Venselaar, H., Shaag, A., Barghuti, F., Reish, O. *et al.* (2009) Mutations in NDUFAF3 (C3ORF60), encoding an NDUFAF4 (C6ORF66)-interacting complex I assembly protein, cause fatal neonatal mitochondrial disease. *Am. J. Hum. Genet.*, **84**, 718–727.
 25. Boulet, L., Karpatis, G. and Shoubridge, E.A. (1992) Distribution and threshold expression of the tRNA(Lys) mutation in skeletal muscle of patients with myoclonic epilepsy and ragged-red fibers (MERRF). *Am. J. Hum. Genet.*, **51**, 1187–1200.
 26. Zeng, X., Barros, M.H., Shulman, T. and Tzagoloff, A. (2008) ATP25, a new nuclear gene of *Saccharomyces cerevisiae* required for expression and assembly of the Atp9p subunit of mitochondrial ATPase. *Mol. Biol. Cell*, **19**, 1366–1377.
 27. Finn, R.D., Tate, J., Mistry, J., Coghill, P.C., Sammut, S.J., Hotz, H.R., Ceric, G., Forslund, K., Eddy, S.R., Sonnhammer, E.L. *et al.* (2008) The Pfam protein families database. *Nucleic Acids Res.*, **36**, D281–D288.
 28. Denoeuf, F., Roussel, M., Noel, B., Wawrzyniak, I., Da Silva, C., Diogon, M., Viscogliosi, E., Brochier-Armanet, C., Couloux, A., Poulain, J. *et al.* (2011) Genome sequence of the stramenopile Blastocystis, a human anaerobic parasite. *Genome Biol.*, **12**, R29.
 29. Thompson, J.D., Higgins, D.G. and Gibson, T.J. (1994) CLUSTAL W: improving the sensitivity of progressive multiple sequence alignment through sequence weighting, position-specific gap penalties and weight matrix choice. *Nucleic Acids Res.*, **22**, 4673–4680.
 30. Guindon, S., Delsuc, F., Dufayard, J.F. and Gascuel, O. (2009) Estimating maximum likelihood phylogenies with PhyML. *Methods Mol. Biol.*, **537**, 113–137.
 31. Abascal, F., Zardoya, R. and Posada, D. (2005) ProtTest: selection of best-fit models of protein evolution. *Bioinformatics*, **21**, 2104–2105.
 32. Sato, A., Kobayashi, G., Hayashi, H., Yoshida, H., Wada, A., Maeda, M., Hiraga, S., Takeyasu, K. and Wada, C. (2005) The GTP binding protein Obg homolog ObgE is involved in ribosome maturation. *Genes Cells*, **10**, 393–408.
 33. Ero, R., Peil, L., Liiv, A. and Remme, J. (2008) Identification of pseudouridine methyltransferase in *Escherichia coli*. *RNA*, **14**, 2223–2233.
 34. Purta, E., Kaminska, K.H., Kasprzak, J.M., Bujnicki, J.M. and Douthwaite, S. (2008) YbeA is the m3Psi methyltransferase RlmH that targets nucleotide 1915 in 23S rRNA. *RNA*, **14**, 2234–2244.
 35. Herold, M., Nowotny, V., Dabbs, E.R. and Nierhaus, K.H. (1986) Assembly analysis of ribosomes from a mutant lacking the assembly-initiator protein L24: lack of L24 induces temperature sensitivity. *Mol. Gen. Genet.*, **203**, 281–287.
 36. Lin, B., Thayer, D.A. and Maddock, J.R. (2004) The Caulobacter crescentum CgtAC protein cosediments with the free 50S ribosomal subunit. *J. Bacteriol.*, **186**, 481–489.
 37. Herold, M. and Nierhaus, K.H. (1987) Incorporation of six additional proteins to complete the assembly map of the 50 S subunit from *Escherichia coli* ribosomes. *J. Biol. Chem.*, **262**, 8826–8833.
 38. Huynen, M., Snel, B., Lathe, W. III and Bork, P. (2000) Predicting protein function by genomic context: quantitative evaluation and qualitative inferences. *Genome Res.*, **10**, 1204–1210.
 39. Szklarczyk, D., Franceschini, A., Kuhn, M., Simonovic, M., Roth, A., Minguez, P., Doerks, T., Stark, M., Muller, J., Bork, P. *et al.* (2011) The STRING database in 2011: functional interaction networks of proteins, globally integrated and scored. *Nucleic Acids Res.*, **39**, D561–D568.
 40. Mehl, R.A., Kinsland, C. and Begley, T.P. (2000) Identification of the *Escherichia coli* nicotinic acid mononucleotide adenyltransferase gene. *J. Bacteriol.*, **182**, 4372–4374.
 41. Orengo, C.A., Michie, A.D., Jones, S., Jones, D.T., Swindells, M.B. and Thornton, J.M. (1997) CATH – a hierarchic classification of protein domain structures. *Structure*, **5**, 1093–1108.

42. Sorek, R., Zhu, Y., Creevey, C.J., Francino, M.P., Bork, P. and Rubin, E.M. (2007) Genome-wide experimental determination of barriers to horizontal gene transfer. *Science*, **318**, 1449–1452.
43. Zybailov, B., Rutschow, H., Friso, G., Rudella, A., Emanuelsson, O., Sun, Q. and van Wijk, K.J. (2008) Sorting signals, N-terminal modifications and abundance of the chloroplast proteome. *PLoS One*, **3**, e1994.
44. Emanuelsson, O., Brunak, S., von Heijne, G. and Nielsen, H. (2007) Locating proteins in the cell using TargetP, SignalP and related tools. *Nat. Protoc.*, **2**, 953–971.
45. Bontell, I.L., Hall, N., Ashelford, K.E., Dubey, J.P., Boyle, J.P., Lindh, J. and Smith, J.E. (2009) Whole genome sequencing of a natural recombinant *Toxoplasma gondii* strain reveals chromosome sorting and local allelic variants. *Genome Biol.*, **10**, R53.
46. Claros, M.G. and Vincens, P. (1996) Computational method to predict mitochondrially imported proteins and their targeting sequences. *Eur. J. Biochem.*, **241**, 779–786.
47. Rorbach, J., Gammage, P.A. and Minczuk, M. C7orf30 is necessary for biogenesis of the large subunit of the mitochondrial ribosome. *Nucleic Acid Res.*
48. Hirano, Y., Ohniwa, R.L., Wada, C., Yoshimura, S.H. and Takeyasu, K. (2006) Human small G proteins, ObgH1, and ObgH2, participate in the maintenance of mitochondria and nucleolar architectures. *Genes Cells*, **11**, 1295–1304.
49. Berger, F., Ramirez-Hernandez, M.H. and Ziegler, M. (2004) The new life of a centenarian: signalling functions of NAD(P). *Trends Biochem. Sci.*, **29**, 111–118.
50. Gordiyenko, Y., Deroo, S., Zhou, M., Videler, H. and Robinson, C.V. (2008) Acetylation of L12 increases interactions in the *Escherichia coli* ribosomal stalk complex. *J. Mol. Biol.*, **380**, 404–414.
51. Yang, Y., Cimen, H., Han, M.J., Shi, T., Deng, J.H., Koc, H., Palacios, O.M., Montier, L., Bai, Y., Tong, Q. *et al.* (2010) NAD⁺-dependent deacetylase SIRT3 regulates mitochondrial protein synthesis by deacetylation of the ribosomal protein MRPL10. *J. Biol. Chem.*, **285**, 7417–7429.
52. Wessels, H.J., Gloerich, J., van der Biezen, E., Jetten, M.S. and Kartal, B. (2011) Liquid chromatography-mass spectrometry-based proteomics of *Nitrosomonas*. *Methods Enzymol.*, **486**, 465–482.
53. Wessels, H.J., Vogel, R.O., van den Heuvel, L., Smeitink, J.A., Rodenburg, R.J., Nijtmans, L.G. and Farhoud, M.H. (2009) LC-MS/MS as an alternative for SDS-PAGE in blue native analysis of protein complexes. *Proteomics*, **9**, 4221–4228.
54. Hooft, R.W., Vriend, G., Sander, C. and Abola, E.E. (1996) Errors in protein structures. *Nature*, **381**, 272.
55. Waterhouse, A.M., Procter, J.B., Martin, D.M., Clamp, M. and Barton, G.J. (2009) Jalview Version 2 – a multiple sequence alignment editor and analysis workbench. *Bioinformatics*, **25**, 1189–1191.